ADVANCED FUNCTIONAL MATERIALS

FULL PAPER

DOI: 10.1002/adfm.200701073

Polydisperse Aggregates of ZnO Nanocrystallites: A Method for Energy-Conversion-Efficiency Enhancement in Dye-Sensitized Solar Cells**

By *Qifeng Zhang, Tammy P. Chou, Bryan Russo, Samson A. Jenekhe,* and *Guozhong Cao**

ZnO films consisting of either polydisperse or monodisperse aggregates of nanocrystallites were fabricated and studied as dye-sensitized solar-cell electrodes. The results revealed that the overall energy-conversion efficiency of the cells could be significantly affected by either the average size or the size distribution of the ZnO aggregates. The highest overall energy-conversion efficiency of ~4.4% was achieved with the film formed by polydisperse ZnO aggregates with a broad size distribution from 120 to 360 nm in diameter. Light scattering by the submicrometer-sized ZnO aggregates was employed to explain the improved solar-cell performance through extending the distance travelled by light so as to increase the light-harvesting efficiency of photoelectrode film. The broad distribution of aggregate size provides the ZnO films with both better packing and an enhanced ability to scatter the incident light, and thus promotes the solar-cell performance.

1. Introduction

ZnO-based dye-sensitized solar cells (DSSCs) have attracted considerable interest during the past several years due to the similarity of the energy band gap and the electron-injection process of ZnO to that of TiO_2.[1,2] Additionally, ZnO can be easily processed into various nanostructures, such as nanoparticles, nanowires, nanotubes, and nanobelts.[3–5] These nanostructures can give rise to many unique features of electron transport or light propagation by either shortening the transfer distance of photoexcited carriers or through light scattering, absorption, or optical confinement. Recent studies on ZnO DSSCs have mostly focused on photoelectrodes with one-dimensional nanostructures such as nanowires or nanotubes in view of the direct electrical pathways through nanowires or nanotubes that can ensure rapid collection of carriers, so as to avoid charge recombination. However, the overall solar-to-electric energy-conversion efficiency is somehow limited by the insufficient surface area of the nanowire or nanotube array.[6–10]

Optical effects generated by nanostructures provide opportunities for increasing the performance of DSSCs in several ways. Light scattering within nanoparticle films is considered as one of the approaches that can make an impact on the photon-capture efficiency, as well as the optical absorption of the photoelectrode in DSSCs. Ferber and Luther,[11] Usami,[12] and Rothenberger et al.[13] have modeled the light scattering in nanocrystalline TiO_2 photoelectrode films admixed with submicrometer-sized TiO_2 particles. It was demonstrated that optical absorption could be significantly enhanced due to the light scattering with the addition of submicrometer-sized TiO_2 particles. However, the specific surface area decreased with the introduction of large-sized particles, and thus an undesired reduction in the dye molecule adsorption would result. TiO_2-based DSSCs have already reached the certified energy-conversion efficiency over 11%.[14] In order to achieve a higher conversion efficiency, it is desirable to introduce large, submicrometer-sized light scatterers into nanocrystalline films without losing the necessary surface area for dye molecule adsorption. Hierarchically structured films with submicrometer-sized aggregates assembled by nanocrystallites appear to be a promising approach to meet such conflicting requirements.

We previously reported a relatively efficient dye-sensitized ZnO solar cell with a conversion efficiency of ~3.5%.[15] The photoelectrode was made of a hierarchically structured film consisting of monodisperse ZnO aggregates ~300 nm in size. In comparison with the efficiency of ~0.3–1.5% reported in the literature for ZnO nanowire electrodes[7,8] and ~0.5–3.4% for ZnO nanoparticle electrodes[16–20], hierarchically structured ZnO films possess the advantage of providing both a huge internal surface area for dye molecule adsorption and the desired submicrometer-sized aggregates as scatterers to enhance the light absorption. In this paper, we employed polydisperse aggregate ZnO films as the photoelectrode of DSSCs, and studied the dependence of the energy-conversion efficiency on the average size and size distribution of aggregates. An

[*] Prof. G. Cao, Dr. Q. Zhang, Dr. T. Chou, B. Russo
Department of Materials Science and Engineering, University of Washington
Seattle, WA 98195 (USA)
E-mail: gzcao@u.washington.edu
Prof. S. A. Jenekhe
Department of Chemical Engineering, University of Washington
Seattle, WA 98195 (USA)

[**] This work was supported by the Air Force Office of Scientific Research (AFOSR-MURI, FA9550-06-1-032) and the Department of Energy. Supporting Information is available online from Wiley InterScience or from the author.

ADVANCED FUNCTIONAL MATERIALS

obviously improved conversion efficiency as high as ~4.4% was achieved for the film consisting of ZnO aggregates with a broad size distribution, which indicated that the optimization of the film structure could result in a significant enhancement of the light scattering of such hierarchically structured films so as to promote the light-harvesting efficiency, as well as the overall energy-conversion efficiency of the cells. The enhancement effect is anticipated to be equally applicable to achieving a higher efficiency for other oxide semiconductor-based DSSCs.

2. Results and Discussion

Polydisperse ZnO aggregates were synthesized via a polyol-mediated precipitation method similar to that reported by Jezequel et al.,[21] and which is briefly described below. Typically, 0.1 M of zinc acetate dihydrate ($ZnAc \cdot 2H_2O$) in diethylene glycol (DEG) was rapidly heated to 160 °C in an oil bath and then kept at this temperature for several hours until a milk-like suspension was formed. Reflux with a water condenser was adopted to prevent solvent loss from evaporation. DEG was chosen here because the hydrolysis of $ZnAc \cdot 2H_2O$ in a DEG medium tends to form colloidal ZnO with a spherical morphology.[22] As-synthesized ZnO aggregates were polydisperse with a wide size distribution, and the average size and size distribution of the aggregates depend on both the $ZnAc \cdot 2H_2O$ concentration and the rate of heating.

To study the influence of the aggregate size on the solar-cell performance and also, as a comparison, monodisperse ZnO aggregates with a narrow size distribution were also synthesized. The method was similar to that which was mentioned above, except that a stock solution was added to induce the nucleation and initial growth of the aggregates.[23] The stock solution contained ZnO nanoparticles with an approximately identical size of about 5 nm and a concentration of 10^{-3} M in DEG. The stock solution was added into the $ZnAc \cdot 2H_2O$-mixed DEG solution when the reaction temperature reached about 130 °C. The as-obtained ZnO aggregates had a uniform diameter and thus are considered as monodisperse aggregates. By adjusting the $ZnAc \cdot 2H_2O$ concentration, the rate of heating, and the amount of stock solution that is added, one can readily control the size of individual aggregates in a wide range.

After cooling down to room temperature, the milk-like colloidal suspensions were subsequently concentrated by firstly using the centrifuge method to separate ZnO aggregates from the polyol solvent, then removing the supernatant, and finally redispersing the precipitate into 5 mL of ethanol with a sonication process for at least 15 min. The photoelectrode films were fabricated by using a drop-cast method to deposit ZnO aggregates on fluorine-doped tin oxide (FTO) glass substrate. The thickness of the films was determined by the number of drops. Finally, the ZnO films were subjected to a heat treatment at 350 °C in air for 1 h to remove the residual organic chemicals from the ZnO surface so as to get an improved contact among those ZnO aggregates, and between the ZnO and dye molecules.[24]

Sensitization of the ZnO films was carried out by immersing the films into a commercial N3 dye for 20 min. The films were then rinsed with ethanol to get rid of excess dye, which was believed to have a negative impact on the transfer of photo-excited electrons.[25,26] After that, the cells were constructed by using a platinum-coated silicon wafer as the counter electrode and the ZnO aggregate films as the working electrode. These two electrodes were placed in parallel and separated by a space with a thickness of 20 μm, where the I^-/I_3^- electrolyte could be injected by capillarity. The measurement of the solar-cell performance was carried out under irradiation of air mass (AM) 1.5 simulated sunlight at 100 mW cm^{-2}.

To study the effects of the average size and size distribution of the aggregates on the solar-cell performance, a number of ZnO films with various structures were prepared and classified into seven groups, named group 1, 2, . . . through 7, in which the films in groups 1 and 2 were made of polydisperse ZnO aggregates and the others only included monodisperse aggregates. Figure 1 shows typical scanning electron microscopy (SEM) images of all these film samples, where Figures 1a through g) correspond to the samples that belong to groups 1 through 7, respectively. One can see that the samples in group 1 consisted of polydisperse ZnO aggregates with diameter varying from 120 to 360 nm, while the samples in group 2 also consisted of polydisperse ZnO aggregates but with the diameter in the region of ~120–310 nm. The other samples were all monodisperse ZnO aggregates with average sizes varying from ~350 nm for group 3, ~300 nm for group 4, ~250 nm for group 5, ~210 nm for group 6, to ~160 nm for group 7. Figure 1h presents a magnified SEM image to reveal that each ZnO aggregate consisted of nanosized crystallites, as further illustrated schematically in Figure 1i.

X-ray diffraction (XRD) analysis was carried out to compare the average size of the nanocrystallites in all the seven group samples. The patterns are shown in Figure 2, where the calculation of nanocrystallite size is based on the Scherer equation.[27] The results reveal that the nanocrystallites in all of the samples had almost the same diameter, of ~12 nm in with a deviation of ±2 nm, which is consistent with that estimated from the high-magnification SEM image in Figure 1h.

The solar-cell performance was characterized by measuring the current–voltage (*I–V*) behaviors of all of the samples when irradiated by a simulated AM 1.5 sunlight source with a power density of $P_{in} = 100$ mW cm^{-2}. Figure 3 illustrates a typical *I–V* curve for one of the samples in group 1, demonstrating the derivation of the open-circuit voltage V_{oc}, the short-circuit current density $I_{sc,}$ and the maximum output power density P_{max}. The overall energy conversion efficiency η and fill factor *FF* can be calculated sequentially by $\eta = P_{max}/P_{in}$ and $FF = P_{max}/(V_{oc} \times I_{sc})$, respectively. The results are summarized in Figure 4, where Figure 4a shows the dependence of the energy-conversion efficiency on the diameter and size distribution of the ZnO aggregates, and Figure 4b indicates a similar trend for the short-circuit current density. It is clear that

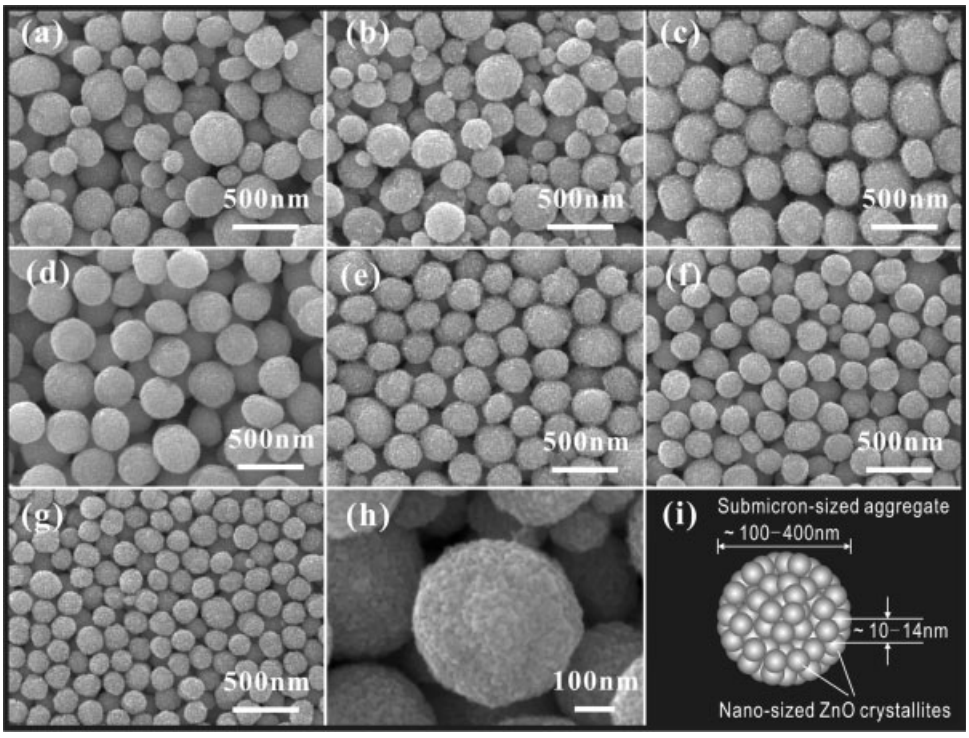

Figure 1. SEM images of hierarchically-structured ZnO films with submicrometer-sized aggregates: (a) and (b) are SEM images of the films consisting of polydisperse aggregates with a size distribution of 120–360 nm and 120–310 nm, respectively; (c) through (g) are SEM images of the films consisting of monodisperse aggregates with average sizes of 350 nm, 300 nm, 250 nm, and 210 nm, respectively; (h) is a magnified SEM image and (i) is a schematic illustration to show the structure of ZnO aggregates formed by closely packed nanocrystallites.

the photoelectrode films with polydisperse ZnO aggregates have both a higher energy-conversion efficiency and a larger short-circuit current density than the films with monodisperse ZnO aggregates. To speak in detail, the electrode films consisting of polydisperse ZnO aggregates with a maximum diameter of 360 nm (samples in group 1) present the highest conversion efficiency of all the samples of 4.4%, approximately 33% higher than the efficiency of 3.3% achieved for the polydisperse ZnO aggregates with the maximum diameter of 310 nm (samples in group 2), and 63% higher than the efficiency of 2.7% for the monodisperse ZnO aggregates with an average size of ~350 nm (samples in group 3). Similarly, the largest short-circuit current density of 21 mA cm^{-2}, achieved for the polydisperse ZnO aggregates with the maximum diameter of 360 nm (samples in group 1), is 40% higher than that of 15 mA cm^{-2} for the polydisperse ZnO aggregates with the maximum diameter of 310 nm (samples in group 2), and 75% higher than that of 12 mA cm^{-2} for the monodisperse ZnO aggregate films (samples in group 3). As for the ZnO films with only monodisperse aggregates, one can see that the decrease in the size of the ZnO aggregates directly results in the degradation of the short-circuit current density from 12 mA cm^{-2} to 7 mA cm^{-2} and the energy-conversion efficiency from 2.7% to 1.5%.

Besides the short-circuit current densities, the open-circuit voltages were also compared to study the influence of aggregate size and size distribution. As expected, we observed almost the same open-circuit voltage, $V_{oc} = 680 \pm 20$ mV, for

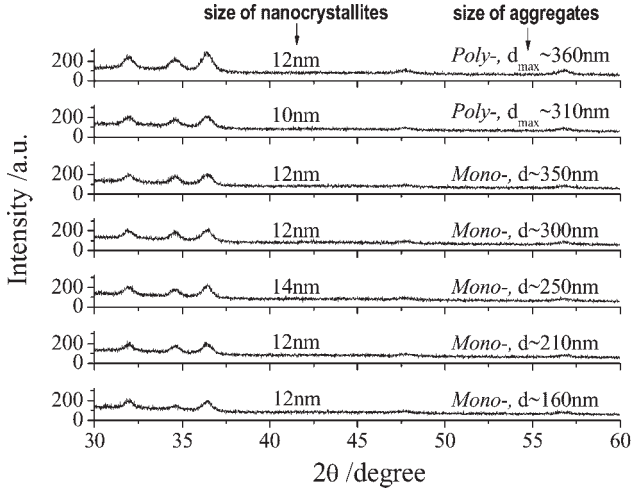

Figure 2. XRD patterns of ZnO films with different sizes and size distributions of aggregates. The nanocrystallite size was calculated by using the Scherer equation.

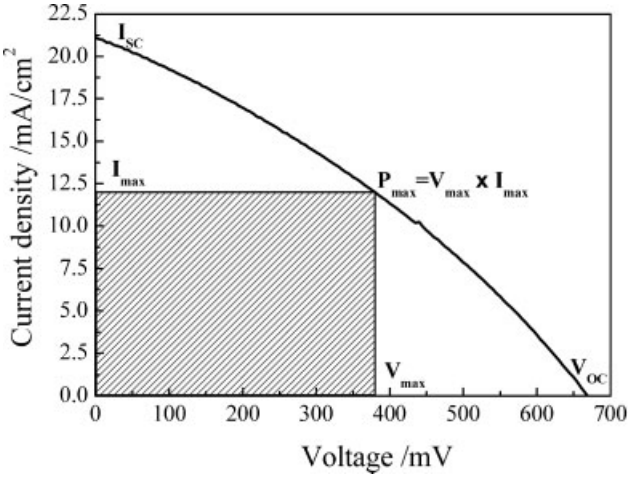

Figure 3. An example of an *I–V* curve for dye-sensitized ZnO solar cells under AM 1.5 irradiation. The square shadow is plotted to illustrate the determination of the maximal power output of the solar cells.

ADVANCED FUNCTIONAL MATERIALS

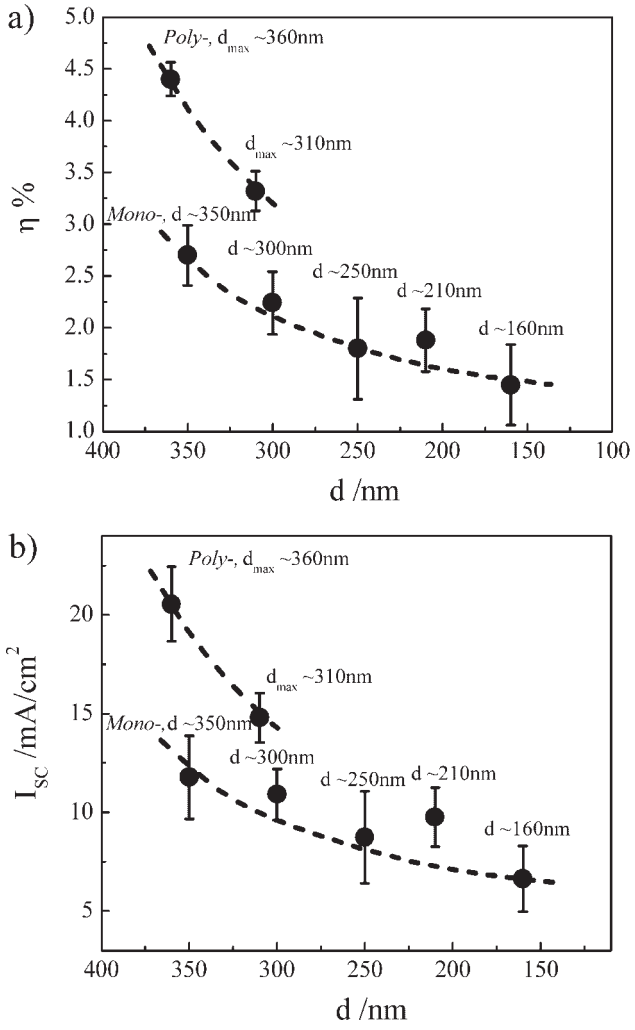

Figure 4. Dependence of (a) overall energy-conversion efficiency and (b) short-circuit current density on the size and size distribution of aggregates in dye-sensitized ZnO solar cells.

all of the ZnO samples in the different groups, considering that the open-circuit voltage was generally determined by the difference between the Fermi level of the oxide semiconductor and the redox potential of the electrolyte. The fill factor is another important parameter that reflects the maximum power output from the solar cell and has a close relation with the geometry structure of each individual cell and the transport mechanism of carriers through the device. However, for all samples with the various dispersities and aggregate sizes, no appreciable difference was observed in the fill factors with an approximately identical value of $FF = 35 \pm 3\%$. The low value of the fill factor, which prevents the ZnO solar cells from achieving an even higher conversion efficiency, may be attributed to the presence of large internal parasitic resistive losses and a serious charge recombination at the ZnO/redox electrolyte interface.[28] That in turn strongly suggests that the combination of ZnO aggregate film and N3 dye or I^-/I_3^- electrolyte is far from optimum and, when considering the fill factor obtained for TiO_2-based DSSCs is ~70%,[29] more efforts are in progress to further improve the performance of this kind of ZnO solar cell.

It appears that only the short-circuit current density is affected by the aggregate size and size distribution, and directly results in the variation of energy-conversion efficiency for the ZnO solar-cell samples in different groups. In the respect that the short-circuit current density in DSSCs mainly depends on the amount of photoexcited electron-hole pairs and the degree of interfacial charge recombination, and for the given photo-electrochemical system including a ZnO film with N3 dye and I^-/I_3^- electrolyte, we can attribute the variation in the short-circuit current density to the difference in either (1) the dye adsorption amount or (2) the light-harvesting efficiency of photoelectrode. The former is decided by the dye adsorption density and the specific surface area of the photoelectrode film. However, the dye adsorption density should be same for all of the samples because of the identical surface chemistry of the ZnO nanocrystallites and the unvaried sensitization process in the present study. Nitrogen sorption isotherms were measured to analyze the specific surface area of the photoelectrode films, and the results revealed that all of the ZnO samples possessed an almost-identical specific surface area of 80 ± 2 m^2 g^{-1}, regardless of the size and size distribution of the aggregates, which corroborated the XRD analysis and SEM observations of the nearly identical nanocrystallite size (12 ± 2 nm) found for all the ZnO samples. Therefore, in the case that both the geometrical area and the film thickness of photoelectrode have been strictly manufactured to be the same, all of the ZnO films in the different groups are believed to adsorb an equal amount of dye molecules. That is to say, the dye adsorption amount is unlikely to be the reason that causes the difference in the short-circuit current density. The latter – the light-harvesting efficiency of photoelectrode film – is basically dependent on the extinction coefficient of the dye and the transport behavior of light within the photoelectrode film. Considering the same dye (N3) is used in this study, it is likely that the film structures with differences in the aggregate size and size distribution can lead to a significant impact on the transport of light within the ZnO films so as to affect the light-harvesting efficiency of photoelectrode.

Figure 5 shows the optical-absorption spectra of the ZnO films with the various structures, and reveals the obvious difference in the absorption intensity for the samples in the different groups. The film with the 160-nm-diameter ZnO nanocrystallites presents a typical absorption, like that obtained for single-crystalline ZnO. The absorption below 385 nm, corresponding to a band-gap energy of 3.2 eV, represents the intrinsic optical absorption of ZnO semiconductor caused by electron transitions from the valence band to the conduction band. Almost no absorption can be observed from this film in the visible region with a wavelength above 385 nm. As the ZnO aggregates of nanocrystallites are gradually formed and the aggregate size becomes increased, the optical absorption of films in the visible region is apparently increased. The most-significant increase occurs in the film that

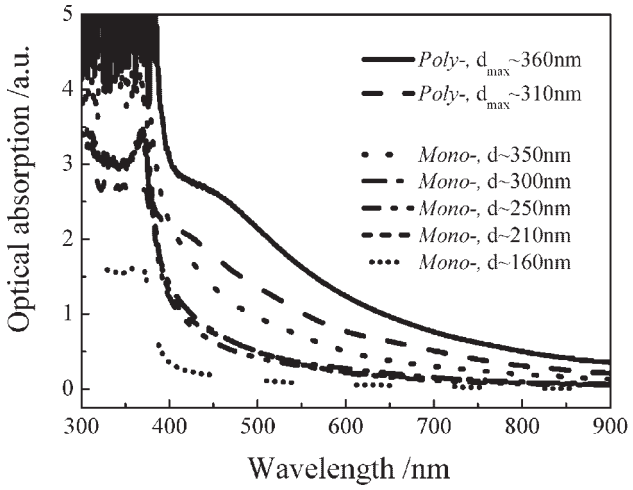

Figure 5. Optical-absorption spectra of the ZnO films consisting of aggregates with different sizes and size distributions.

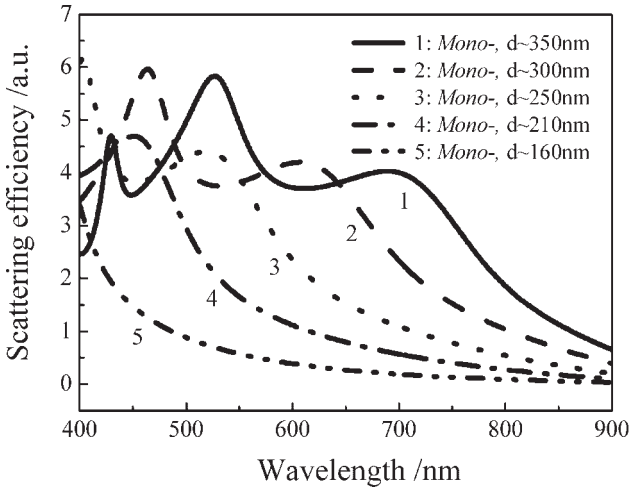

Figure 6. Theoretically calculated light-scattering efficiency as a function of wavelength when the scatterer size is changed from 160 nm to 350 nm, corresponding to the actual size of the ZnO aggregates in the present study.

belongs to group 1 consisting of polydisperse ZnO aggregates with a broad size distribution from 120 to 360 nm in diameter. The result implies that the enhancement in optical absorption originates from the aggregation of ZnO nanocrystallites and is proportional to the average size of the monodisperse aggregates or the dispersion degree of polydisperse aggregates in size distribution. This phenomenon can be explained by the light scattering of submicrometer-sized ZnO aggregates, which may change the transport direction of light travelled in the films and thereby attenuate the light that transmits through the films.

Light scattering by spherical particles can be analytically described by Mie resonance theory, in which the scattering efficiency, Q_{sca}, is given by Equation (1):[30,31]

$$Q_{sca} = \frac{2}{x^2}\sum_{n=1}^{\infty}(2n+1)\left(|a_n|^2 + |b_n|^2\right) \quad (1)$$

where $x = 2\pi r/\lambda$ is the size parameter, r is the radius of a dielectric sphere, λ is the wavelength of light, and a_n and b_n are the complex Mie coefficients that can be calculated as:

$$a_n = \frac{\psi'_n(mx)\psi_n(x) - m\psi_n(mx)\psi'_n(x)}{\psi'_n(mx)\zeta_n(x) - m\psi_n(mx)\zeta'_n(x)} \quad (2)$$

$$b_n = \frac{m\psi'_n(mx)\psi_n(x) - \psi_n(mx)\psi'_n(x)}{m\psi'_n(mx)\zeta_n(x) - \psi_n(mx)\zeta'_n(x)} \quad (3)$$

where, m is the refractive index of a dielectric sphere, and ψ and ζ are the Riccati–Bessel functions.[32,33] Figure 6 presents the results of a calculation of the scattering efficiency for monodisperse ZnO aggregates with the diameter varied from 160 nm to 350 nm, corresponding to the samples in group3 through 7. During the calculation, the wavelength-dependent refractive index of ZnO was obtained from the literature.[34] From Figure 6, one can see that the scattering efficiency is a function of the incident wavelength and aggregate size. In the wavelength range of ~400–900 nm, the sample consisting of large aggregates with 350 nm diameter possesses the largest scattering efficiency, whereas the sample with the 160 nm aggregates has the lowest scattering efficiency. This is reasonable because a resonant scattering most likely occurs when the size of the aggregates is comparable with the wavelength of the incident light. The calculated results of the optical-scattering efficiency for monodisperse aggregates agree very well with the experimental optical-absorption spectra as shown in Figure 5, indicating the light-scattering mechanism of absorption enhancement in the ZnO films consisting of submicrometer-sized aggregates.

The light scattering influences the transport behavior of light through changing the path and/or extending the distance of light travelled within the photoelectrode film, and thus the light-harvesting efficiency gets improved due to the increased probability of interaction between the photons and the dye molecules that adsorb on the ZnO nanocrystallites. Compared with the films that contain only monodisperse aggregates, the films with polydisperse aggregates present an apparent virtue in the enhancement of the optical absorption and energy-conversion efficiency, as shown in Figure 5 and 4a, respectively. Polydisperse aggregates likely lead to a disordered structure when they are packed in a random way to form the film. Many studies in the literature have demonstrated that a less-ordered medium is more effective in the generation of multiple scattering to light and the formation of closed loops for light confinement.[35–37] The broader distribution of aggregate sizes means an increased irregularity in the assembly of

ADVANCED FUNCTIONAL MATERIALS

film, resulting in the fact that, as mentioned above, the samples in group 1 consisting of polydisperse aggregates with a size distribution in quite a large range possess the highest conversion efficiency. Another reason that polydisperse aggregates exhibit excellent ability for the enhancement of optical absorption as well as solar-cell efficiency is the different-sized aggregates that can cause light scattering in a wide wavelength range. Besides the effect of generating a strong scattering to light, polydisperse aggregates are also thought to be good at the formation of network interconnections so as to create a photoelectrode film with a closely packed structure, which offers more pathways for the transport of electrons in the film.

3. Conclusions

We report the synthesis of ZnO films with polydisperse aggregates and have studied the impact of the size and size distribution of ZnO aggregates on the overall conversion efficiency of dye-sensitized ZnO solar cells. The results indicate that polydisperse aggregates with a large average size or broad size distribution could result in an obvious enhancement in the optical absorption and light-harvesting efficiency of photoelectrode films. This is because of the light scattering, which was generated by submicrometer sized aggregates with a size dimension comparable to the wavelength of the incident light, which could extend the travelling distance of light within the photoelectrode film. Compared to the conversion efficiency below 2.7% for the films with the 350 nm monodisperse ZnO aggregates and the efficiency of 3.3% for the films including polydisperse aggregates but with a relatively narrow size distribution, the films that consisted of polydisperse aggregates with a broad size distribution from 120 to 360 nm presented a significantly improved solar-cell conversion efficiency as high as 4.4%. The promotion of solar-cell performance was also demonstrated to originate in part from the polydisperse aggregates being able to provide the film with a closely packed structure, which was of benefit to the transport of electrons in the photoelectrode film.

4. Experimental

ZnO aggregates were synthesized through hydrolysis of 0.9855 g of zinc acetate dihydrate in 45 mL of diethylene glycol at 160 °C. Reflux with water cooling was employed to prevent the solvent evaporating. A rapid heating at 10 °C min^{-1} was used to fabricate the polydisperse ZnO aggregates with a broad size distribution, while a rate of 5 °C min^{-1} was used to obtain the polydisperse aggregates with the relatively narrow size distribution. To synthesize monodisperse ZnO aggregates, an amount of stock solution was added into the reaction solution when the temperature reached 130 °C and meanwhile the zinc acetate was completely dissolved. The stock solution was made of 5 nm ZnO nanoparticles prepared via a sol–gel approach and dispersed in the diethylene glycol with a concentration of about 10^{-3} M. Corresponding to the average sizes of 350 nm, 300 nm, 250 nm, 210 nm and 160 nm for monodisperse ZnO aggregates, respectively, 0.5 mL, 1 mL, 5 mL, 10 mL and 20 mL of stock solution were added. The as-obtained milk-like colloidal suspension was centrifuged at 3000 rpm for 5 h to separate the ZnO aggregates from the solvent. The supernatant was removed and the precipitate was washed with ethanol several times by a repeated sonication-centrifugation process. The precipitate was finally redispersed into 5 mL of ethanol for further use.

Films with an active area of 1.0 cm^2 were deposited on FTO-covered glass substrates using a drop-cast method. The film thickness was fabricated to be about 10 μm, identical for all the samples by exactly controlling the added drops. After the films became dry, they were heat treated at 350 °C in air for 1 h to dispose of the residual chemicals on the ZnO surface and also to improve the contact between the film and substrate, as well as that between the ZnO aggregates.

For device build-up, the film samples were firstly sensitized through immersing in ruthenium-based N3 dye (Solterra Fotovoltaico SA, Switzerland) with a concentration of 0.5 mM in ethanol for 20 min. The samples were then rinsed with ethanol to remove additional dye on the surface. To assemble the solar cells, dye-sensitized ZnO film was employed to serve as the working electrode and a platinum-coated silicon wafer as the counter electrode. The two electrodes were placed face to face at a distance of ~40 μm with two pieces of thin membrane that were put at each edge of the electrode as the spacer. I^-/I_3^--based liquid electrolyte, which contained 0.3 M lithium iodide, 0.06 M I_2, 1.0 M tetrabutylammonium iodide and 0.5 M 4-*tert*-butylpyridine in acetonitrile was introduced into the space between the two electrodes by capillarity.

The solar-cell performance was characterized in an HP 4155A programmable semiconductor parameter analyzer, while the samples were illuminated by AM 1.5 simulated sunlight with the power density of 100 ± 3 mW cm^{-2}. The open-circuit voltage, the short-circuit current density, and the maximum output power density could be directly obtained from the as-recorded current–voltage curve, and the fill factor and overall conversion efficiency were accordingly calculated as to their definition. For each film structure with given aggregate size or size distribution, four samples were prepared and tested independently to derive the statistical mean of energy-conversion efficiency and short-circuit current density. The data were used for plotting Figure 4.

The optical-absorption spectra were measured using an ultraviolet-visible-near infrared (UV-VIS-NIR) spectrophotometer (Perkin Elmer Lambda 900). The films were fabricated on glass substrates with an identical thickness for all the samples, and these samples suffered the same heat treatment process as those for solar-cell testing. A blank glass slide was used as a reference to eliminate the influence of the glass substrate on the optical absorption.

Received: September 15, 2007
Revised: November 21, 2007
Published online: May 20, 2008

[1] C. Bauer, G. Boschloo, E. Mukhtar, A. Hagfeldt, *J. Phys. Chem. B* **2001**, *105*, 5585.
[2] A. Furube, R. Katoh, T. Yoshihara, K. Hara, S. Murata, H. Arakawa, M. Tachiya, *J. Phys. Chem. B* **2004**, *108*, 12583.
[3] Z. L. Wang, *J. Phys.: Condens. Matter* **2004**, *16*, R829.
[4] Z. Y. Fan, J. G. Lu, *J. Nanoscience Nanotechnology* **2005**, *5*, 1561.
[5] A. B. Djurišić, Y. H. Leung, *Small* **2006**, *2*, 944.
[6] M. Law, L. E. Greene, J. C. Johnson, R. Saykally, P. D. Yang, *Nat. Mater.* **2005**, *4*, 455.
[7] J. B. Baxter, E. S. Aydil, *Appl. Phys. Lett.* **2005**, *86*, 053114.
[8] A. D. Pasquier, H. H. Chen, Y. C. Lu, *Appl. Phys. Lett.* **2006**, *89*, 253513.
[9] K. S. Leschkies, R. Divakar, J. Basu, E. Enache-Pommer, J. E. Boercker, C. B. Carter, U. R. Kortshagen, D. J. Norris, E. S. Aydil, *Nano Lett.* **2007**, *7*, 1793.
[10] A. B. F. Martinson, J. W. Elam, J. T. Hupp, M. J. Pellin, *Nano Lett.* **2007**, *7*, 2183.

[11] J. Ferber, J. Luther, *Sol. Energy Mater. Sol. Cells* **1998**, *54*, 265.
[12] a) A. Usami, *Chem. Phys. Lett.* **1997**, *277*, 105. b) A. Usami, *Sol. Energy Mater. Sol. Cells* **2000**, *64*, 73.
[13] G. Rothenberger, P. Comte, M. Grätzel, *Sol. Energy Mater. Sol. Cells* **1999**, *58*, 321.
[14] M. Grätzel, *Inorg. Chem.* **2005**, *44*, 6841.
[15] T. P. Chou, Q. F. Zhang, G. E. Fryxell, G. Z. Cao, *Adv. Mater.* **2007**, *19*, 2588.
[16] H. Rensmo, K. Keis, H. Lindström, S. Södergren, A. Solbrand, A. Hagfeldt, S. E. Lindquist, L. N. Wang, M. Muhammed, *J. Phys. Chem. B* **1997**, *101*, 2598.
[17] X. Sheng, Y. Zhao, J. Zhai, L. Jiang, D. Zhu, *Appl. Phys. A. – Mater. Sci. Process.* **2007**, *87*, 715.
[18] P. Suri, M. Panwar, R. M. Mehra, *Mater. Sci. - Poland* **2007**, *25*, 137.
[19] P. Suri, R. M. Mehra, *Sol. Energy Mater. Sol. Cells* **2007**, *91*, 518.
[20] An efficiency of ~5% obtained from ZnO nanoparticle films was reported by Keis et al. However, considering that a very particular method with a pressure of 1000 kg cm^{-2} was used to fabricate the films and the measurement was carried out using one tenth (10 mW cm^{-2}) of the AM 1.5 (1 sun) irradiance, the result is not included for comparison in this study. One can see: a) K. Keis, E. Magnusson, H. Lindstrom, S.-E. Lindquist, A. Hagfeldt, *Sol. Energy Mater. Sol. Cells* **2002**, *73*, 51. b) K. Keis, C. Bauer, G. Boschloo, A. Hagfeldt, K. Westermark, H. Rensmo, H. Siegbahn, *J. Photochemistry Photobiology A: Chem.* **2002**, *148*, 57.
[21] D. Jezequel, J. Guenot, N. Jouini, F. Fievet, *Mater. Sci. Forum* **1994**, *152*, 339.
[22] L. Poul, S. Ammar, N. Jouini, F. Fievet, F. Villain, *J. Sol–Gel Sci. Technol.* **2003**, *26*, 261.
[23] E. W. Seelig, B. Tang, A. Yamilov, H. Cao, R. P. H. Chang, *Mater. Chem. Phys.* **2003**, *80*, 257.
[24] See Section S1 in Online Supporting Information.
[25] K. Keis, J. Lindgren, S. E. Lindquist, A. Hagfeldt, *Langmuir* **2000**, *16*, 4688.
[26] K. Westermark, H. Rensmo, H. Siegbahn, K. Keis, A. Hagfeldt, L. Ojamae, P. Persson, *J. Phys. Chem. B* **2002**, *106*, 10102.
[27] B. D. Cullity, *Elements of X-Ray Diffraction*, 2nd ed., Addison-Wesley Publishing Company, New York **1978**, p. 281.
[28] See Section S2 in Online Supporting Information.
[29] M. K. Nazeeruddin, P. Péchy, T. Renouard, S. M. Zakeeruddin, R. Humphry-Baker, P. Comte, P. Liska, L. Cevey, E. Costa, V. Shklover, L. Spiccia, G. B. Deacon, C. A. Bignozzi, M. Grätzel, *J. Am. Chem. Soc.* **2001**, *123*, 1613.
[30] C. F. Bohren, D. R. Huffman, *Absorption and Scattering of Light by Small Particles*, Wiley-Interscience, New York **1983**.
[31] S. M. Scholz, R. Vacassy, J. Dutta, H. Hofmann, *J. Appl. Phys.* **1998**, *83*, 7860.
[32] M. Abramowitz, I. A. Stegun, *Handbook of Mathematical Functions: With Formulas, Graphs, and Mathematical Tables*, Dover Pub., New York **1965**.
[33] H. Du, *Appl. Opt.* **2004**, *43*, 1951.
[34] X. W. Sun, H. S. Kwok, *J. Appl. Phys.* **1999**, *86*, 408.
[35] D. S. Wiersma, P. Bartolini, A. Lagendijk, R. Righini, *Nature* **1997**, *390*, 671.
[36] H. Cao, J. Y. Xu, D. Z. Zhang, S. H. Chang, S. T. Ho, E. W. Seelig, X. Liu, R. P. H. Chang, *Phys. Rev. Lett.* **2000**, *84*, 5584.
[37] X. H. Wu, A. Yamilov, H. Noh, H. Cao, E. W. Seelig, R. P. H. Chang, *J. Opt. Soc. Am. B* **2004**, *21*, 159.